Hindawi
Contrast Media & Molecular Imaging
Volume 2022, Article ID 3921362, 8 pages
https://doi.org/10.1155/2022/3921362

Research Article

Preparation and MRI Study of HER2-Targeted Bimodal Molecular Probe Gd-Cy5.5-Pertuzumab for Thyroid Cancer

Hongda Tian,[1] **Jinren Liu**,[1] **Zhengrong Xie**,[1] **Zhongyuan Li**,[2] **and Chunxiang Li**[2]

[1]*Department of Molecular Imaging, School of Medical Technology, Qiqihar Medical University, Qiqihar, China*
[2]*Department of Molecular Imaging, The First Affiliated Hospital of Qiqihar Medical University, Qiqihar, China*

Correspondence should be addressed to Zhongyuan Li; m15946506063@163.com and Chunxiang Li; lichunxiang@qmu.edu.cn

Received 18 October 2022; Revised 2 December 2022; Accepted 2 December 2022; Published 30 December 2022

Academic Editor: Guillermina Ferro Flores

Purpose. A bimodal nanoprobe for thyroid cancer targeting human epidermal growth factor receptor 2 (HER2) was synthesized by coupling the magnetic resonance contrast agent Gd^{3+} with the fluorescent dyes Cy5.5 and pertuzumab as a preliminary study of Gd-Cy5.5-pertuzumab in magnetic resonance and fluorescence imaging. *Methods*. The bifunctional chelate p-SCN-Bn-1,4,7,10-tetraazacyclododecane-1,4,7,10-tetraacetic-acid (DOTA) was dissolved in deionized water, added to pertuzumab solution, and stirred overnight at room temperature to obtain the product DOTA pertuzumab. 1,2-dichloroethane and N-hydroxysuccinimide were added to activate the carboxyl group on DOTA. After 0.5 hr of activation, the amino fluorescent dye Cy5.5 was further added to react with it to synthesize the intermediate product Cy5.5-DOTA-pertuzumab. Finally, we added $GdCl_3$-$6H_2O$ and placed it in a magnetic stirrer for 6 hr before the unreacted substance was removed by dialysis to obtain Gd-Cy5.5-pertuzumab. Following that, the hydrated particle size and zeta potential of the nanoprobe were measured by particle size analyzer, the fluorescence spectrum by a fluorescence detector, the infrared spectrum by the infrared analyzer, the cytotoxicity by CCK-8 method, the relaxation rate by Niumai small nuclear magnetic field, and the binding ability of HER2 to thyroid cancer 8505C by laser confocal microscope. Nanoprobes were injected into a subcutaneous thyroid cancer nude mouse model through the tail vein, and *in vivo* MRI and near-infrared (NIR) fluorescence imaging were performed. Finally, the nude mice were dissected and hematoxylin and eosin (HE) staining of pathological tissues was performed to evaluate the imaging performance of the prepared bimodal probes. *Results*. The synthesized bimodal probe Gd-Cy5.5-pertuzumab had a hydrodynamic size of 131.34 ± 9.43 nm and zeta potential of -31.73 ± 6.24 mV with a significant absorption peak at 685 nm. The relaxation rate of the probe was 46.53 $mM^{-1}\,s^{-1}$, which was determined by Niumai small nuclear magnetism, and the T_1 signal intensity increased gradually with the concentration of the probe. Laser confocal microscopy showed that HER2 was mainly expressed in cell membranes. *In vitro* and *in vivo* experiments indicated that the probe had low cytotoxicity. MRI and small animal fluorescence imaging of tumor-bearing nude mice showed that the probe could clearly image tumor tissue. *Conclusion*. The bimodal probe Gd-Cy5.5-pertuzumab was successfully synthesized with good stability, which can specifically bind to target cells *in vivo* and has good magnetic resonance/fluorescence imaging performance.

1. Introduction

Thyroid cancer is a common malignant tumor of the endocrine system in China, and its incidence is increasing year by year [1]. At present, the etiology of thyroid cancer regardless of type has not been fully understood and the treatment plan is not yet clear. The prognosis for the treatment is not encouraging [2], despite the fact that surgery, radiation, chemotherapy, and other complete treatment procedures are typically performed. The emphasis of interest has shifted more and more recently to molecular probes and focused therapies. The use of imaging methods reveals biological-specific molecules at the tissue, cellular, and subcellular levels, reflecting the changes at the molecular level in the living state, and leading to qualitative and quantitative research of their biological behavior and imaging [3]. Since molecular probes and targeted therapy are the hope of today's diagnosis and treatment of thyroid cancer, more extensive and in-depth basic experiments and clinical research are needed to develop a more accurate diagnosis and treatment methods. The human epidermal growth factor receptor 2 (HER2, also known as HER), galectin-1, and Src homology2 (SH2)domain-containg protein tyrosine phosphatase, among others, are the particular targets of thyroid cancer molecular

probes at the moment. HER2 can be expressed on the cytoplasmic membrane and can be specifically recognized by pertuzumab injected into the body, resulting in a conformational change and tight binding [4]. Therefore, pertuzumab, as an important targeting component, has been widely used in the synthesis of tumor-targeted tracers. It has been demonstrated in the literature that HER2 can be exploited as a possible target for thyroid cancer since the expression rate of HER2 in thyroid cancer is 44%, which is much higher than the expression rate of 4% in benign thyroid lesions [5]. The advantage of near-infrared fluorescence imaging is that it can reduce the attenuation and scattering of optical signals by hemoglobin, water, and fat in the organism to a certain extent, so that the detection depth can be increased in imaging. The benefits of gadolinium in magnetic resonance imaging are unsurpassed by those of other contrast agents, which are particular imaging agents for nuclear magnetic resonance [6]. Gd^{3+} is a positive contrast agent, with strong paramagnetic properties, showing high signal in T_1 imaging, easy modification, good biocompatibility, and can chelate with various substances to form stable complexes, image spatial resolution, and signal-to-noise ratio higher. The simultaneous use of magnetic resonance imaging and fluorescence imaging, which combines the benefits of both imaging modalities, has emerged as a new trend in the development of molecular imaging [7, 8]. Dual-modality imaging can complement the advantages of imaging modalities, efficient disease diagnosis, and reduced radiation risks [9]. Given this, this experiment would prepare and synthesize a HER2-targeted magnetic resonance/fluorescence dual-modal nanoparticle Gd-Cy5.5-pertuzumab, to detect the characterization of the probe, observe its imaging performance, and explore the feasibility of nanoprobe imaging *in vivo*.

2. Materials and Methods

2.1. Materials. Following materials were employed in the study: particle size analyzer (NICOMP 380 ZLS); fluorescence spectrophotometer (RF-5301PC); quasi-dual-beam UV–vis spectrophotometer (UV-3802); nuclear magentic resonance (NMR) contrast medium relaxation rate analysis and imaging system (NM120); multifunctional enzyme labeling instrument (Safire2); ion acidity meter (PHS-3C); ultrasonic cleaner (XM-3200UVF); heat collecting magnetic stirrer (DF-101S); One ten thousandth balance (QUINTIX65-1CN); 3.0T MRI (Philips); IVIS Lumina Series (PerkinElmer, USA); laser confocal microscope (LSM710); Dulbecco's modified eagle medium (DMEM) cell culture medium; Cy5.5, pertuzumab, 1,2-dichloroethane (EDC)-HCl, N-hydroxysuccinimide (NHS); cells purchased from Shanghai Cell Bank of Chinese Academy of Sciences; cells cultured in DMEM, Roswell Park Memorial Institute 1640 medium at 37°C with 5% CO_2 incubator, diethylenetriamine pentaacetate (DTPA).

2.2. Synthesis of Gd-Cy5.5-Pertuzumab. We diluted pertuzumab in deionized water at a concentration of 10 mg/ml, added sodium bicarbonate to adjust the pH of the solution to 8.4, and added bifunctional chelation according to the molar ratio of pertuzumab to p-SCN-Bn-1,4,7,10-tetraazacyclododecane-1,4,7,10-tetraacetic-acid (DOTA) of 1 : 10 [10, 11]. The solution was mixed and placed in an ultrasonic oscillator for 15 min for complete dispersion before being taken out and placed in a magnetic stirrer and shaken the reaction overnight at room temperature. The unreacted material was removed from the reactant with a 30 kDa ultrafiltration tube to obtain the product DOTA-pertuzumab. EDC and NHS were added, and the carboxyl group was fully activated after 30 min of reaction. We weighed 20 mg $GdCl_3$-$6H_2O$ and 100 μg Cy5.5 into the above solution to mix and react for 6 hr. The product was ultrafiltered with a 30 kDa ultrafiltration tube to remove unreacted $GdCl_3$-$6H_2O$ and Cy5.5 to obtain the product Gd-Cy5.5-pertuzumab, and at the same time, the intermediate product Gd-DOTA-Cy5.5 was prepared as a control group.

2.3. Statistical Analysis. SPSS 21.0 software was used for statistical analysis. All experiments were repeated at least three times, and all data were expressed as mean ± standard deviation. The *t*-test analysis was used to compare the two pairs, and $P < 0.05$ was considered statistically significant.

3. Characterization of Gd-Cy5.5-Pertuzumab

3.1. Inductively Coupled Plasma (ICP) Gd Element Content Determination. A fivefold dilution of the nanoprobe solution was taken into the instrument, a pink flame appears in the observation window, the temperature of the semiconductor refrigeration atomizer was kept constant at 2°C, and then the sample was detected.

3.2. Measurement of Transmission Electron Microscope Size. We took an appropriate amount of Gd-Cy5.5-pertuzumab solution and dispersed the ultrasonic probe with water as a dispersant. Then, we used a dropper to take a drop of suspension on the copper mesh. After drying, the shape and particle size of the synthesized probe were observed under the transmission electron microscope.

3.3. Measurement of Hydrodynamic Dimension and Zeta Potential. One-hundred microliters of Gd-Cy5.5-pertuzumab solution was taken, diluted with deionized water, transferred to an Eppendorf tube via pipette, and sonicated for 15 min to completely disperse the prepared nanoprobes. The hydrodynamic size and zeta potential of the nanoprobe Gd-Cy5.5-pertuzumab were detected in the color dish.

3.4. Characterization of Optical Properties. Two milliliters of the prepared sample solution was taken and transferred into a standard cuvette through a pipette. The ultraviolet adsorption spectrum of the synthesized pertuzumab, Gd-DOTA, and Gd-Cy5.5-pertuzumab NPs was detected using a UV–vis spectrometer. The surface functional groups of the probes were detected by Fourier transform infrared spectroscopy.

3.5. Determination of Relaxation Rate. Three probes, namely, Gd-Cy5.5-pertuzumab, Gd-DOTA-pertuzumab, and Gd-DTPA, were diluted with deionized water to obtain different concentration gradients: 0.1–0.5 (Gd^{3+} mM). After dilution, 1 ml of different concentrations of Gd was taken and placed in Eppendorf tubes. One at a time was taken and placed in a

Newmai minispec NMR analyzer. The magnet probe was meso 60–60 mm and the sequence was IR. Parameters: SF (MHz): 23, O1 (Hz): 317,507.42, P1 (μs): 12.00, TD: 1,024, premagnification: 1, TW (ms): 3,000.000, P2 (μs): 24.00, number of times inversion: 25, SW (kHz): 100, radio frequency delay (ms): 0.080, RG1 (dB): 10.0, digital gain: 3, and NS: 4. The relaxation rates of the three probes were calculated and compared.

3.6. Cytotoxicity Test. To evaluate the effect of the probe on cells, their toxicity was assayed using the cell counting kit-8 (CCK-8) method. Thyroid cancer 8505C cells, SW579 cells, and MIN6 cells in good logarithmic growth phase were selected, removed from the culture medium, washed three times with phosphate-buffered saline (PBS), and then digested with trypsin. After centrifugation and counting, cells were seeded in a 96-well plate, 100 μl of cell suspension was added to each well, and the 96-well plates were filled with PBS around the plate and the humidity of the 96-well plates was maintained to facilitate evaporation before being incubated for 24 hr at 37°C and 5% CO_2. We added 100 μl of culture medium containing different concentrations of probes to the 96-well plate, respectively, continued to culture for 24 hr, added 100 μl of CCK-8 solution to each well of the 96-well plate, incubated for 2–3 hr, used a microplate reader to detect the value at 450 nm, and calculated toxicity of probes at different concentrations in cells.

3.7. Confocal Laser Imaging. The binding state of the probe to cells and the expression of HER2 was detected using confocal laser microscopy. 8505C cells, SW579 cells, and MIN6 cells were cultured in a 20 mm glass-bottom cell culture dish for 24 hr and the cell status was observed by fluorescence microscopy. The cells were rinsed three times with PBS and incubated overnight at 37°C in the dark, and then the cells were rinsed three times again with PBS and fixed with 4% paraformaldehyde for 30 min at room temperature. Then, rabbit monoclonal antibody-HER2 antibody was added and incubated at 4°C for 24 hr. At room temperature, an anti-rabbit IgG antibody was added and incubated for 1 hr. Finally, 4′,6-diamidino-2-phenylindole (DAPI) was added for staining for 15 min for the localization of cell nuclei, and the uptake of three cells was observed by a laser confocal microscope.

8505C cells were selected and cultured in a 20 mm glass-bottom cell culture dish, and washed three times with PBS. The targeted probe Gd-Cy5.5-pertuzumab and the nontargeted probe Gd-DOTA-Cy5.5 were added at 37°C in the dark and incubated overnight, and following, rinsed three times with PBS and fixed with 4% paraformaldehyde for 30 min at room temperature. Then, rabbit monoclonal antibody-HER2 antibody was added and incubated at 4°C for 24 hr. The binding of targeted probes and nontargeted probes to cells was observed.

4. Animal Experiment

4.1. Establishment of Animal Models. Twelve 4-week-old nude mice were randomly selected from the cage, 8505C cells were injected into the right armpit of the nude mice at a cell concentration of 2×10^7/ml, and each nude mouse was injected with 200 μl. The growth was about 10 days, and the tumor diameter was about 10 mm. Animal research has been reviewed and approved by the Animal Ethics Committee (QMU-AECC-2022-86).

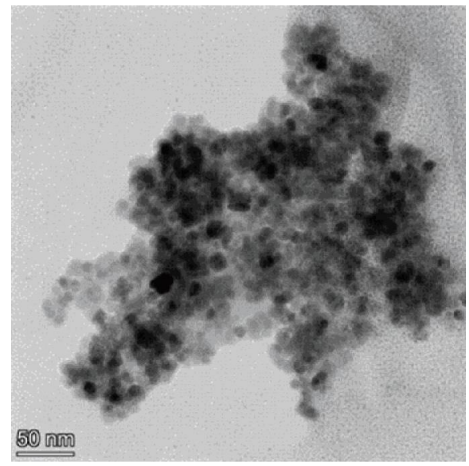

Figure 1: Gd-Cy5.5-pertuzumab transmission electron microscope.

4.2. Magnetic Resonance Imaging. Six tumor-bearing nude mice were taken, anesthetized by abdominal injection, and placed in a 3.0T Philips MRI fingertip joint coil for a T_1-weighted plain scan. After injecting the probe (0.05 mmol/kg) into the tail vein, T_1-weighted scans were performed at four time periods (0, 1, 1.5, and 4 hr). The changes in tumor signal intensity were observed.

4.3. Fluorescence Imaging. Another six tumor-bearing nude mice were taken, anesthetized at different time points, and injected with probes (0.05 mmol/kg) Gd-Cy5.5-pertuzumab and Gd-DOTA-Cy5 through the tail vein. The tumor fluorescence intensity and change trends of the two nanoprobes at 0, 2, 4, 6, and 24 hr, five time points were observed using the fluorescence imager.

4.4. In Vivo Cytotoxicity Studies. Sprague Dawley (SD) rats were randomly divided into two groups, one group of seven rats and the other group of eight rats. The experimental group was injected 1 ml of NaCl solution (100 ml/kg) to the nanoprobe Gd-Cy5.5-pertuzumab through the tail vein, and the control group was injected 1 ml of NaCl solution through the tail vein. Fourteen days later, 3 ml of blood was collected from the orbital venous plexus of rats and placed in sodium heparin centrifuge tubes. After centrifugation for 10 min, the supernatant was taken. The indexes of alanine aminotransferase (ALT), aspartate aminotransferase (AST), alkaline phosphatase (ALP), blood urea nitrogen (BUN), and creatinine (Cr) were measured by a biochemical detector.

4.5. HE Staining. The nude mice were executed by intraperitoneal injection of excessive pentobarbital sodium, and the main organs, heart, liver, spleen, and kidney, were taken for hematoxylin and eosin (HE) staining, and those injected with Gd-Cy5.5-pertuzumab were the experimental group. Physiological saline was the control group. The tissues of the experimental group were observed for necrosis and damage.

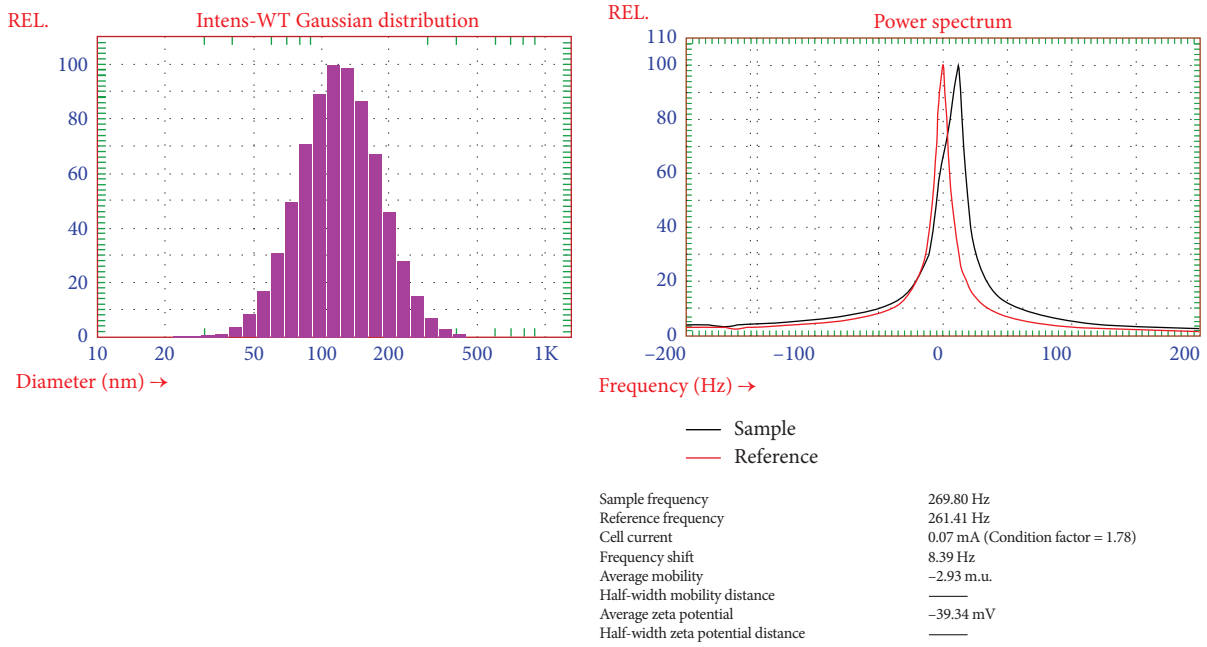

FIGURE 2: (a) Gd-Cy5.5-pertuzumab nanoprobe hydration particle size; (b) Gd-Cy5.5-pertuzumab nanoprobe zeta potential.

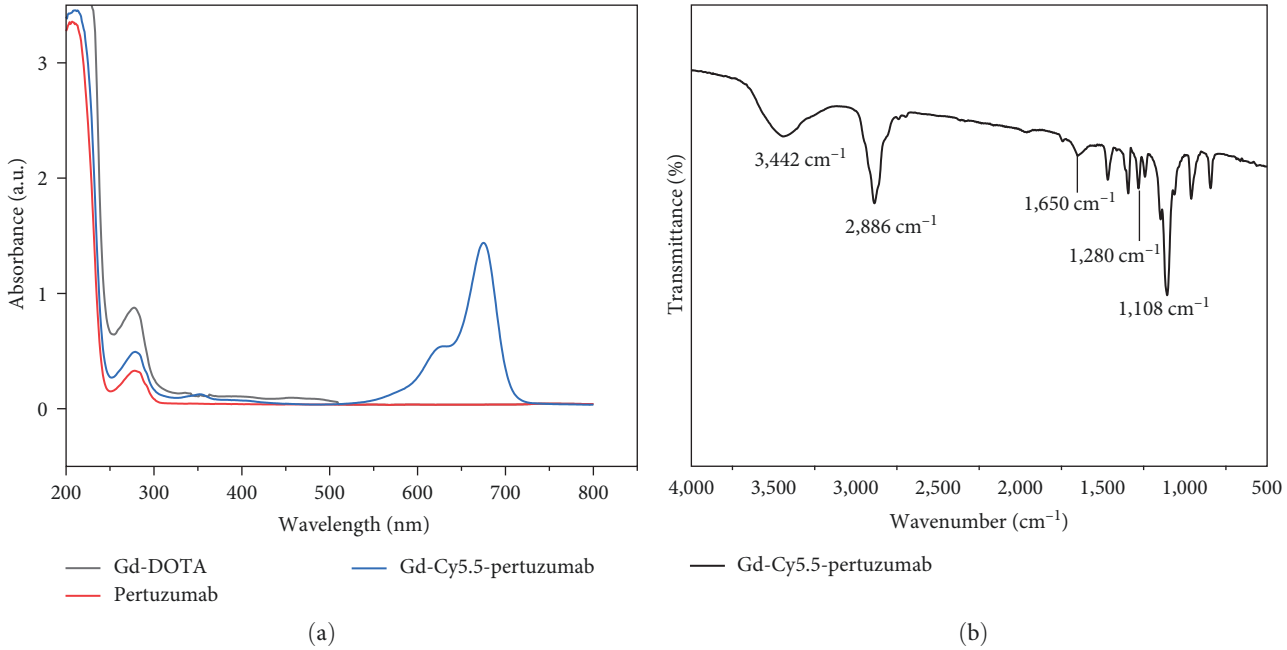

FIGURE 3: (a) UV–vis absorption spectra of Gd-DOTA, pertuzumab, and Gd-Cy5.5-pertuzumab; (b) infrared spectra of Gd-Cy5.5-pertuzumab.

5. Results

5.1. Characterization of Nanoprobes. After fivefold dilution by ICP, the content of Gd element was detected as 196 μg/ml. Transmission electron microscopy results showed that the nanoprobe Gd-Cy5.5-pertuzumab was circular in shape and uniform in size (Figure 1). The hydrated particle size of Gd-Cy5.5-pertuzumab was 131.34 ± 9.43 nm, with a narrow probe distribution size and good dispersion (Figure 2(a)). The zeta potential was -31.73 ± 6.24 mV (Figure 2(b)), indicating the stability of the composite. The larger the positive value or the smaller the negative value, the higher its stability [12].

5.2. Fluorescence. After the coupling of pertuzumab, Gd-DOTA, and Cy5.5, the UV absorption peaks of Cy5.5 and pertuzumab all appeared in Gd-Cy5.5-pertuzumab, indicating that the probe was successfully coupled (Figure 3(a)).

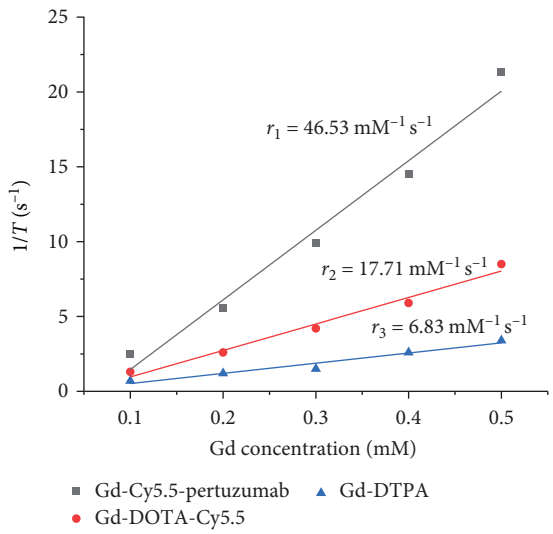

Figure 4: Gd-Cy5.5-pertuzumab, Gd-DOTA-pertuzumab, Gd-DTPA relaxation rate.

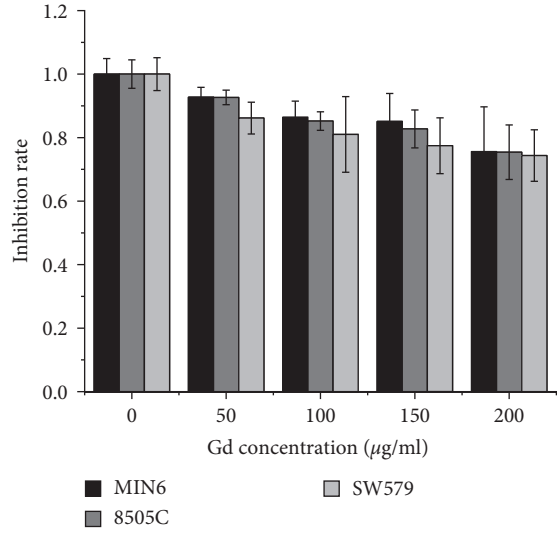

Figure 5: Gd-Cy5.5-pertuzumab cytotoxicity.

Table 1: Blood chemistry results of Sprague Dawley rats injected with Gd-Cy5.5-pertuzumab nanoparticles.

	ALT (U/l)	AST (U/l)	ALP (U/l)	BUN (mmol/l)	Cr (μmol/l)
Gd-Cy5.5-pertuzumab ($n=8$)	52.50 ± 21.78	106.63 ± 24.47	219.50 ± 57.04	8.70 ± 2.27	35.38 ± 7.27
Control ($n=7$)	57.14 ± 19.13	108.86 ± 20.19	215.43 ± 47.43	7.93 ± 1.14	32.29 ± 8.08
P	0.670	0.852	0.884	0.431	0.449

The infrared spectrum showed that there was an absorption peak at 3,442 cm^{-1}, which was the stretching vibration peak of OH, the absorption peak at 2,886 cm^{-1} was the saturated C–H stretching vibration peak, the absorption peak at 1,650 cm^{-1} was the amide bond I band formed by pertuzumab and DOTA, the absorption peak at 1,280 cm^{-1} may be the stretching vibration peak of C–N, and the absorption peak at 1,108 cm^{-1} may be the stretching vibration peak of C–O–C. It indicated that the group coupling of the nanoprobe was successful (Figure 3(b)).

5.3. In Vitro Magnetic Resonance Imaging and Relaxation Rate. Nanoprobes Gd-Cy5.5-pertuzumab, Gd-DOTA-pertuzumab, and Gd-DTPA: 0.1, 0.2, 0.3, 0.4, 0.5 (Gd^{3+} mM) probe T_1 relaxation times were measured by Newman NMR at different concentrations. The relaxation rates $r_1 = 46.53$, $r_2 = 17.71$, and $r_3 = 6.83$ mM^{-1} s^{-1} were obtained by linear fitting with Origin software. The relaxation rate of the targeted probe group was significantly higher than that of the nontargeted group (Figure 4).

5.4. Biosafety of the Probe. The cytotoxicity of Gd-Cy5.5-pertuzumab was detected by CCK-8 assay (Figure 5). The results of the three cell experiments showed that the cell activity without the probe was 100%. The highest activity of MIN6 cells and the lowest activity of SW579 cells were observed after the addition of the probe. The activity of the three cells decreased with the increase of the probe concentration. After incubation at 200 μg/ml for 24 hr, the activity of Gd was still greater than 75%, and the dose used was higher than *in vivo* animal experiments, indicating that the probe has low toxicity to cells. There were no significant differences in ALT, AST, ALP, BUN, and Cr compared with the control group, indicating that the prepared probes were not significantly toxic *in vivo* (Table 1).

5.5. Laser Confocal. The HER2 antibody in thyroid cancer 8505C cells and SW579 cells was expressed in the cell membrane and cytoplasm by laser confocal microscopy, showing green color and blue color in the nucleus by DAPI staining. Among them, the fluorescence of HER2 antibody in 8505C cells was much higher than in SW579 cells, while almost no green fluorescence was observed on the surface of islet MIN6 cells, indicating that HER2 was highly expressed in anaplastic thyroid carcinoma 8505C cells, but not in MIN6 cells (Figure 6).

Under laser confocal microscopy, the HER2 antibody in 8505C cells was expressed mainly in the cell membrane, which was green and the nuclei of DAPI-stained cells were blue. The targeted probe Gd-Cy5.5-pertuzumab and the nontargeted probe Gd-DOTA-Cy5.5 were added to two plates containing 8505C cells respectively. After excitation by the excitation light source, the red light was shown to be clearer after binding of the targeting probe to the cells, which indicated that targeted probe binds specifically to the cell, while the nontargeted probe binds to a weaker degree, implying that its targeting was poor (Figure 7).

5.6. In Vivo Magnetic Resonance Imaging. Tumor-bearing nude mice were anesthetized and performed a T_1 plain scan. A mass-like hypodense shadow with a uniform signal was seen in the right axilla. After injection of targeting probe

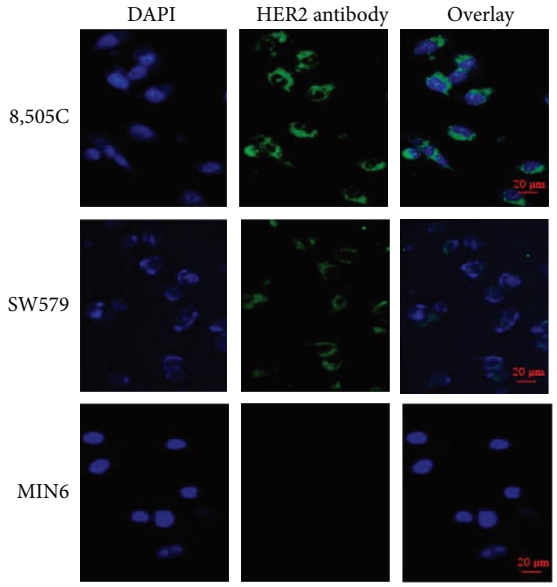

Figure 6: Laser confocal fluorescence imaging of different cells (20 μm).

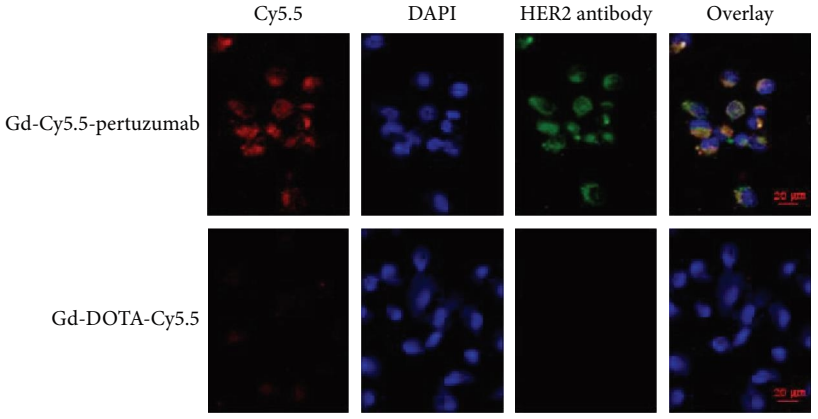

Figure 7: Laser confocal immunofluorescence imaging (20 μm).

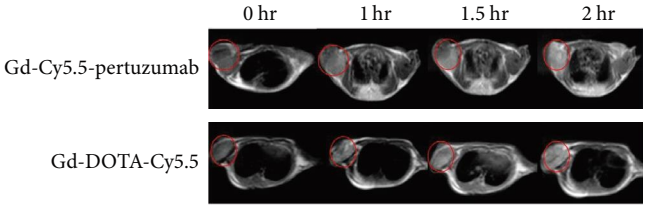

Figure 8: *In vivo* magnetic resonance imaging.

Gd-Cy5.5-pertuzumab and nontargeting probe Gd-DOTA-Cy5.5 via tail vein, T_1-weighted imaging was performed at 1, 1.5, and 2 hr, respectively. It can be seen that the T_1 signal of the axillary mass was low at 0 hr, and the signal of the mass gradually increased between 0 and 2 hr, with a clear boundary with the surrounding tissue. The signal enhancement degree of the targeted probe group was significantly higher than that of the nontargeted group (Figure 8).

5.7. In Vivo Fluorescence Imaging. After anesthetized with anesthetics, 100 μl of the probe was injected through the tail vein, imaged with a small animal fluorescence imager, and imaged at 0, 1, 2, 4, and 24 hr. It can be seen that the fluorescence of nude mice injected with targeted probe Gd-Cy5.5-pertuzumab is stronger than the nontargeted probe Gd-DOTA-Cy5.5, and the fluorescence concentration in the targeted group is higher at 2 hr of tumor. The fluorescence intensity began to weaken at 4 hr and gradually disappeared at 24 hr (Figure 9).

5.8. HE Staining. After executing nude mice, they were sectioned and stained. It showed that the heart, liver, spleen, and kidney of the experimental group were normal without pathological changes, and there was no significant difference between the experimental group and the control group (Figure 10).

6. Discussion

HER2 is a promising biomarker of thyroid cancer, which is expressed in the tumor cell membrane [13]. HER2, widely

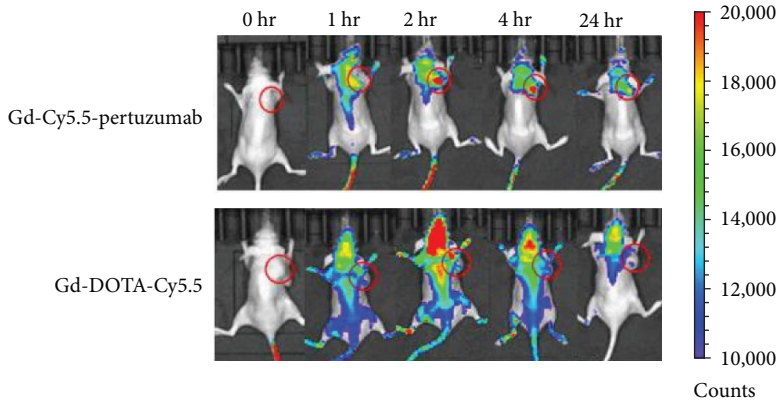

Figure 9: Fluorescence imaging of small animals in nude mice.

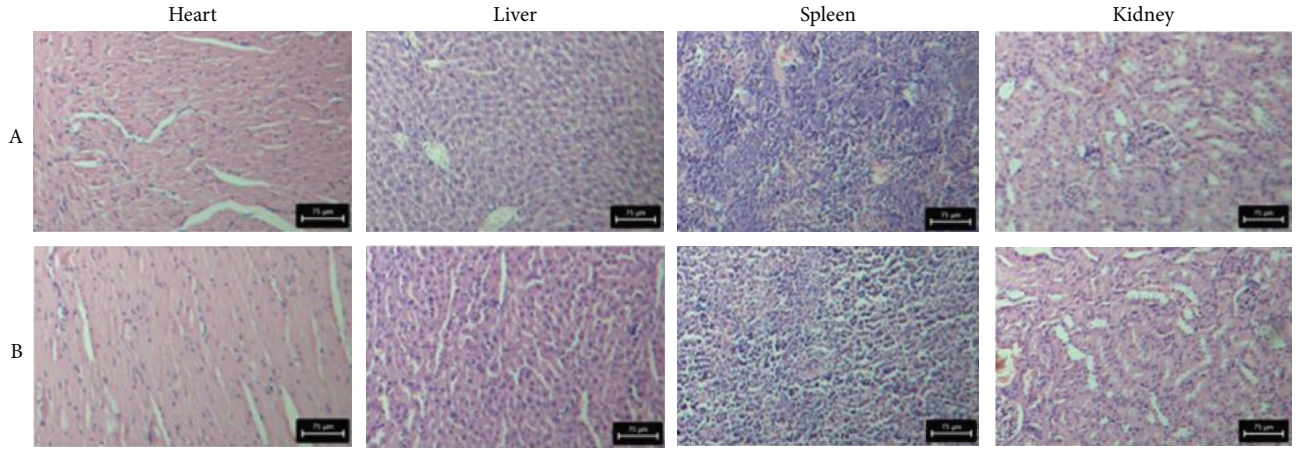

Figure 10: (a) Experimental group; (b) control group.

employed in the early diagnosis and treatment of malignancies, plays a significant role in the process of tumor metastasis [14, 15]. Pertuzumab is used as a targeted substance for specific binding with HER2, which can achieve specific binding with HER2 receptor on the surface of tumor cells. The combination of pertuzumab with magnetic resonance and fluorescent materials can increase the binding rate of the prepared probe to the target cells. The bimodal imaging with the probe is helpful for the noninvasive diagnosis of HER2-positive thyroid cancer. Therefore, the study of a new dual-mode probe is of great significance for the early diagnosis of thyroid cancer. With the development of technology over the past several years, molecular imaging has advanced quickly, and molecular probes have steadily taken the place of core technologies in molecular imaging [16]. Molecular imaging technology can be used to dynamically monitor the tumor. The majority of targeted probe investigations for thyroid cancer, both domestically and internationally, are single mode, with radionuclide probes receiving greater attention than magnetic resonance and fluorescence studies. The preparation method of bimodal targeted probes connecting Gd and Cy5.5 by using pertuzumab as the targeting group is simple and easy to operate. Magnetic resonance imaging is considered one of the most powerful cell tracking tools because of its deep tissue, high spatial resolution, and noninvasive. Optical imaging can only penetrate a few millimeters of tissue, but is inexpensive, sensitive, and time-resolving. Therefore, these two imaging methods complement each other and provide more information for the diagnosis of thyroid cancer. This study synthesized bimodal nanoprobes to monitor the expression of HER2, so as to realize the early diagnosis of thyroid cancer and provide new ideas for the early warning of thyroid cancer. The nanoprobe prepared in this study was wrapped with magnetic resonance contrast agent Gd^{3+}, fluorescent dye Cy5.5, and targeting substance pertuzumab, which had the dual advantages of magnetic resonance and fluorescence. According to its imaging analysis and characterization, the produced nanoprobe exhibited high biocompatibility, homogeneous shape, and good dispersion. The probe uses the widely used magnetic resonance T_1 imaging agent Gd^{3+}, which avoids the risk that superparamagnetic iron oxide particles can be easily inhaled by the liver by using the magnetic resonance T_2 imaging agent. The cytotoxicity results showed that the nanoprobe had little cytotoxicity on cells, and the biochemical indicators further confirmed that the injection measurement of the probe solution in the experimental group had no significant effect on the liver and kidney function of rats. These results all showed that the toxicity of Gd-Cy5.5-pertuzumab has little effect on living animals. The relaxation rate of the nanoprobe Gd-Cy5.5-pertuzumab was 46.53 $mM^{-1}\,s^{-1}$, which was higher than that of

Gd-DTPA without the target material. The traditional Gd-DTPA has no targeting and a low relaxation rate. By coupling pertuzumab and Cy5.5, the nanoprobe effectively increases the targeting of the probe and improves the relaxation performance. The nanoprobe has a hydrodynamic size of 131.34 ± 9.43 nm and a zeta potential of -31.73 ± 6.24 mV. The potential size can reflect the stability of the nanoprobe, the larger the absolute value of the value, the more stable the probe system is and the less likely it is to aggregate [17]. *In vitro* experiments showed that the signal intensity of the probe increased with the increase of concentration, and the signal changed significantly, which proved that the nanoprobe Gd-Cy5.5-pertuzumab could be used as a T_1 positive contrast agent. In *in vitro* cell experiments, laser confocal showed that the second antibody appeared green after incubation, which was mainly expressed on the cell membrane. The probe contains Cy5.5, so it showed a red light and was mainly expressed on the cell membrane. The fusion image showed that red and green were located on the membrane surface. The targeted probe exhibits more red light than the nontargeted probe, which suggests that the targeted probe is particularly linked to cells, according to a comparison of the two probes, namely, Gd-Cy5.5-pertuzumab and Gd-DOTA-Cy5.5. *In vivo* fluorescence showed that the fluorescence intensity at the tumor site of nude mice in the targeted probe group gradually increased at 0–2 hr and reached the peak at 2 hr. Within 0–2 hr of the probe being administered, *in vivo* magnetic resonance imaging revealed that the signal at the tumor steadily increased. HE staining results showed that the prepared nanoprobe Gd-Cy5.5-pertuzumab had no significant pathological changes in the main organs compared with the normal control group. In conclusion, the magnetic resonance/fluorescence dual-mode probe Gd-Cy5.5-pertuzumab synthesized in this experiment was characterized by uniform size, stable properties, low cytotoxicity, and good targeting with HER2-specific binding on tumor cell membrane. The synthesized probe showed high signal and high fluorescence intensity tumors in magnetic resonance imaging and near-infrared fluorescence imaging, which can provide early warning for the early diagnosis of thyroid cancer, and is expected to provide guidance for the treatment plan of patients.

Data Availability

The data used to support the findings of this study are included within the article.

Conflicts of Interest

The authors declare that they have no conflicts of interest.

Funding

This study was funded by the Natural Science Foundation of Heilongjiang Province (LH2022H109).

References

[1] J. Qing, X. Shi, and S. Liu, "New advances in research on etiology of thyroid cancer," *Chinese Journal of Otolaryngology-Head and Neck Surgery*, vol. 55, no. 7, pp. 711–715, 2020.

[2] X. Li, W. Jiang, Y. Zhong et al., "Advances of circular RNAs in thyroid cancer: an overview," *Biomedicine & Pharmacotherapy*, vol. 140, Article ID 111706, 2021.

[3] C. J. Palestro, "Molecular imaging of infection: the first 50 years," *Seminars in Nuclear Medicine*, vol. 50, no. 1, pp. 23–34, 2020.

[4] N. Iqbal and N. Iqbal, "Human epidermal growth factor receptor 2 (HER2) in cancers: overexpression and therapeutic implications," *Molecular Biology International*, vol. 2014, Article ID 852748, 9 pages, 2014.

[5] W. Wei, D. Jiang, Z. T. Rosenkrans et al., "HER2-targeted multimodal imaging of anaplastic thyroid cancer," *American Journal of Cancer Research*, vol. 9, no. 11, pp. 2413–2427, 2019.

[6] N. T. Nghia, E. Tinet, D. Ettori et al., "Gadolinium/terbium hybrid macromolecular complexes for bimodal imaging of atherothrombosis," *Journal of Biomedical Optics*, vol. 22, no. 7, Article ID 076604, 2017.

[7] N. Kamaly, A. D. Miller, and J. D. Bell, "Chemistry of tumour targeted T1 based MRI contrast agents," *Current Topics in Medicinal Chemistry*, vol. 10, no. 12, pp. 1158–1183, 2010.

[8] A. Gupta, L. de Campo, L. J. Waddington et al., "Towards advanced paramagnetic nanoassemblies of highly ordered interior nanostructures as potential MRI contrast agents," *New Journal of Chemistry*, vol. 41, no. 7, pp. 2735–2744, 2017.

[9] J. F. Liao, X. W. Wei, B. Ran, J. R. Peng, Y. Qua, and Z. Y. Qian, "Polymer hybrid magnetic nanocapsules encapsulating IR820 and PTX for external magnetic field-guided tumor targeting and multifunctional theranostics," *Nanoscale*, vol. 9, no. 7, pp. 2479–2491, 2017.

[10] R. Hernandez, H. Sun, C. G. England et al., "CD146-targeted immunoPET and NIRF imaging of hepatocellular carcinoma with a dual-labeled monoclonal antibody," *Theranostics*, vol. 6, no. 11, pp. 1918–1933, 2016.

[11] J. Zhang, *Nuclide Labeling and SPECT/CT Molecular Imaging of HER2 Targeted Biomolecules*, Shanghai Normal University, Shanghai, 2018.

[12] X. R. Li, Z. Wei, and D. K. Su, "Integrin $\alpha v\beta 3$ preparation and characterization of a targeted bimodal molecular probeUSPIO-cy5.5-cRGD," *Journal of Clinical Radiology*, vol. 36, no. 3, pp. 425–429, 2017.

[13] J.-B. Zhang, Y.-J. Wang, and D. Li, "Clinical significance of detection of serum and thyroid tissue markers in female patients with Hashimoto's thyroiditis," *Maternal and Child Health Care of China*, vol. 36, no. 8, pp. 1878–1881, 2021.

[14] M. M. Moasser, "The oncogene HER2: its signaling and transforming functions and its role in human cancer pathogenesis," *Oncogene*, vol. 26, pp. 6469–6487, 2007.

[15] Y. Jin, B. Liu, M. H. Younis et al., "Next generation molecular imaging of thyroid cancer," *Cancers*, vol. 13, no. 13, Article ID 3188, 2021.

[16] M. Liu, D. W. Leng, and X. M. Fan, "Progress in multimodal molecular imaging," *Chinese Journal of Medical Imaging*, vol. 26, no. 6, pp. 471–475, 2018.

[17] X. Liu, N. Zheng, Y.-N. Shi, J. Yuan, and L. Li, "Thyroid hormone induced angiogenesis through the integrin $\alpha v\beta 3$/protein kinase D/histone deacetylase 5 signaling pathway," *Journal of Molecular Endocrinology*, vol. 52, no. 3, pp. 245–254, 2014.